Electronic Supplementary Information (ESI)

A Mesoporous (3,36)-connected *Txt*-type Metal-Organic Framework Constructed by A Naphthyl-embedded Ligand Exhibiting High CO$_2$ Storage and Selectivity

Zhiyong Lu[a], Jianfeng Zhang[a]*, Haiyan He[a], Liting Du[b]*, Cheng Hang[c]

[a] College of Mechanics and Materials, Hohai University, Nanjing 210098, China
[b] Advanced Analysis and Testing Center, Nanjing Forestry University, Nanjing 210037, China.
[c] State Key Laboratory of Coordination Chemistry, Nanjing University, Nanjing 210093, China

Table of contents

SECTION S1. Experimental Section

Preparation of Ligand, 5,5'-((6,6'-((pyridine-3,5-dicarbonyl)bis(azanediyl))bis(2-naphthoyl))bis(a - zanediyl))diisophthalic acid, H_4PANAD. Into a flask flushed with N_2, anhydrous pyridine-3,5-dicarboxylic acid, (1 g, 6 mmol) was placed and 40 mL of thionyl chloride was added. The mixture was stirred and refluxed over night until it got transparent. After cooling down, the excess $SOCl_2$ was evaporated and the resulting white solid was further washed with n-hexane to remove the residue of $SOCl_2$. Then the fluffy white solid was dissolved in anhydrous dimethylacetamide (DMA) and the solution was cooled with an ice bath. Into the solvent, DMAP (4-(dimethylamino)pyridine, 0.1 g, 0.8 mmol) was added followed by addition of 6-amino-2-naphthoic acid (2.36 g, 12.6 mmol). After stirring for 1 h at 0 °C and 48 h at room temperature, the reaction solution was poured into a large excess of water. The precipitated solids were filtered off and washed repeatedly with hot methanol. The wet solid was dried in a vacuum oven at 100 °C to yield pure 6,6'-((pyridine-3,5-dicarbonyl)bis (azanediyl))di-2-naphthoic acid (H_2NL) as a brown powder (2.8 g, 92.3 % yield). ^1H NMR (500MHz, DMSO-d6, δ ppm): 13.00 (brs, 2H, −COOH), 10.95 (s, 2H, −CO−NH−), 9.36 (d, 2H, Py−H), 8.944 (t, 1H, Py−H), 8.58 (s, 4H, Ar−H), 8.17 (s, 1H, Ar−H), 8.14 (s, 1H, Ar−H), 7.99 (s, 4H, Ar−H), 7.95 (d, 1H, Ar−H), 7.92 (d, 1H, Ar-H). 1 g H_2NL was used as the starting material and repeat similar step as mentioned above, by adding 5-aminoisophthalic acid (0.761 g, 4.2 mmol) instead of 6-amino-2-naphthoic acid. Finally, 1.5 g H_4PANAD was obtained in brown solid with the yield of 91.2 %. ^1H NMR (500MHz, DMSO-d6, δ ppm): 13.31 (brs, 4H, −COOH), 10.99 (d, 1H, −CO−NH−), 10.88 (t, 2H, −CO−NH−), 10.77 (s, 1H, −CO−NH−), 9.43 (brs, 2H, Py−H), 8.98 (t, 1H, Py−H), 8.78 (s, 1H, Ar−H), 8.75 (s, 4H, Ar−H), 8.63 (d, 2H, Ar−H), 8.40 (d, 1H, Ar−H), 8.27 (d, 2H, Ar−H), 8.25 (d, 2H, Ar−H), 8.20 (d, 1H, Ar−H), 8.14 (d, 1H, Ar−H), 8.08 (s, 2H, Ar−H), 7.98 (d, 1H, Ar−H), 7.94 (d, 1H, Ar−H). IR (KBr, cm^{-1}): 3067, 1700, 1685, 1653, 1605, 1541, 1491, 1430, 1394, 1332, 1284, 1236, 1198, 906, 809, 760, 729.

Preparation of HHU-1, $[Cu_2(PANAD)(H_2O)]_n$. A solution of $Cu(NO_3)_2 \cdot 3H_2O$ (19.3 mg, 0.08 mmol), H_4PANAD (9.98 mg, 0.012 mmol) and 0.05 ml of concentrated HCl were mixed in the solvent of DMF/H_2O (V/V=5/1) (2 ml). The mixture was sealed in a Pyrex tube and heated to 55°C for 5 days. The green octahedral crystals obtained were filtered and washed with DMF. The yield of the reaction based upon the weight of the solvent-free material is ~ 50.6 % based upon H_4PANAD. Selected IR (KBr, cm^{-1}): 2932, 1654, 1559, 1541, 1507, 1490, 1436, 1375, 1281, 1199, 1097, 903, 814, 775, 731. Anal. Calcd. (Found) for activated HHU-1 [C45 H25 Cu2 N5 O12]: C, 56.56 (56.31) H, 2.83 (3.17) N, 7.33 (8.02).

SECTION S2. Crystal structure

Table S1. Crystal Data for HHU-1.

	HHU-1
CCDC number	1523860
Empirical formula	$C_{45} H_{27} Cu_2 N_5 O_{13}$
Formula weight	972.82
crystal system	Cubic
Space group	*Im-3m*
a [Å]	41.4734(4)
b [Å]	41.4734(4)
c [Å]	41.4734(4)
α [deg]	90
β [deg]	90
γ [deg]	90
V [Å^3]	71336(2)
Z	24
T [K]	173(2)
ρ_{calc} [g cm^{-3}]	0.544
R1, wR2^a [$I>2\sigma(I)$]	0.0442; 0.1774
R1, wR2^a [all data]	0.0797; 0.1755

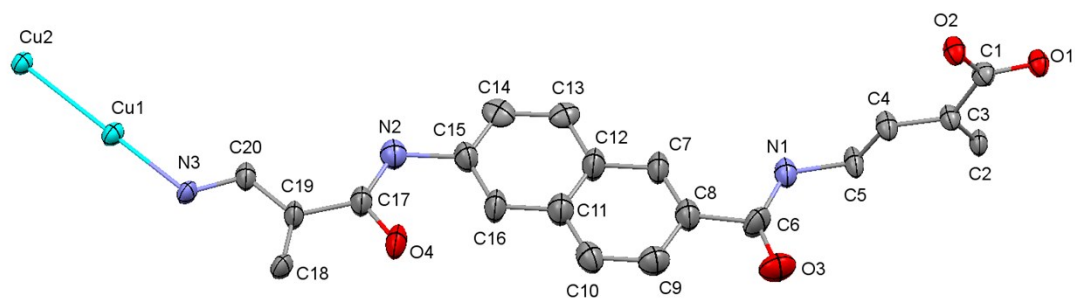^{a} R1 = $\Sigma||F_o| - |F_c||/|F_o|$; wR2 = $[\Sigma w(\Sigma F_o^2 - F_c^2)^2/\Sigma w(F_o^2)^2]^{1/2}$
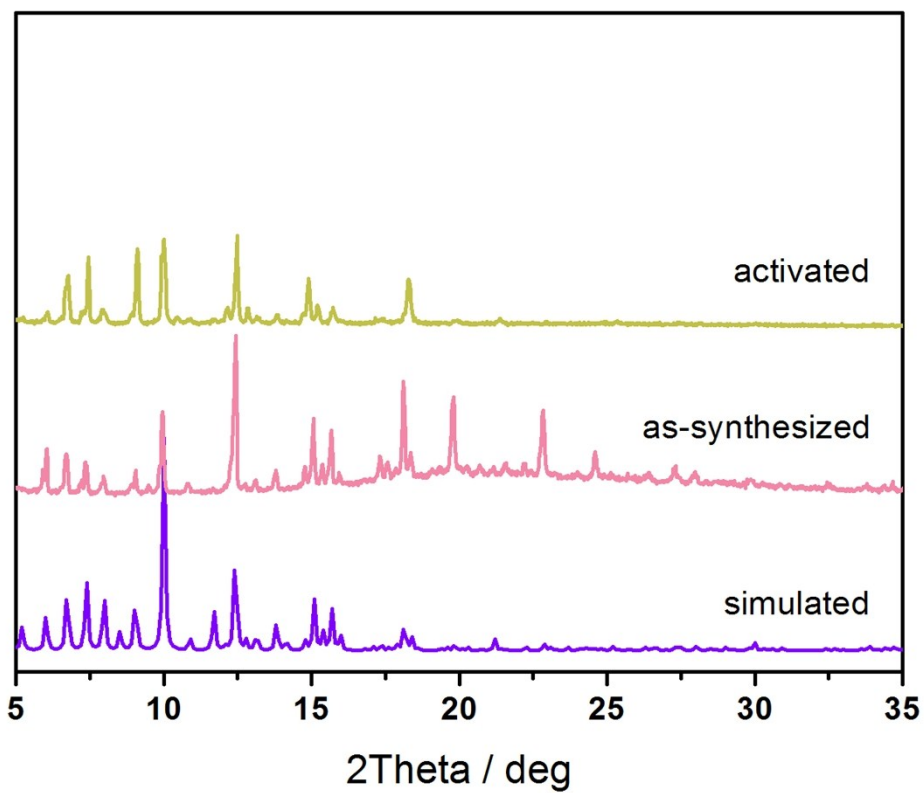
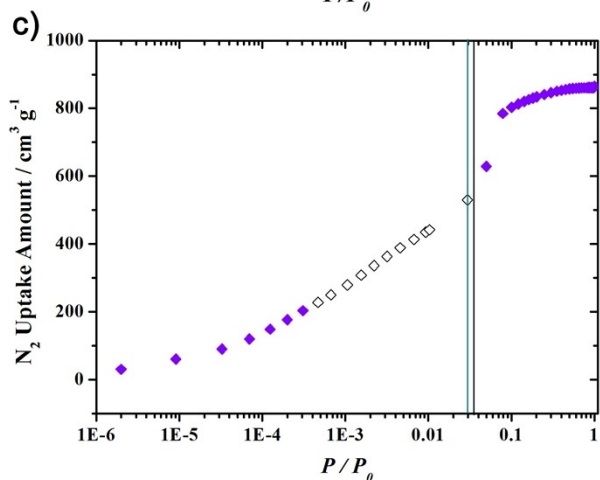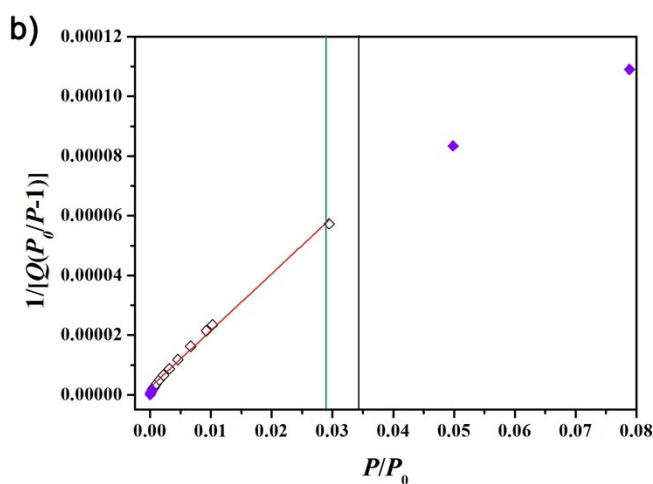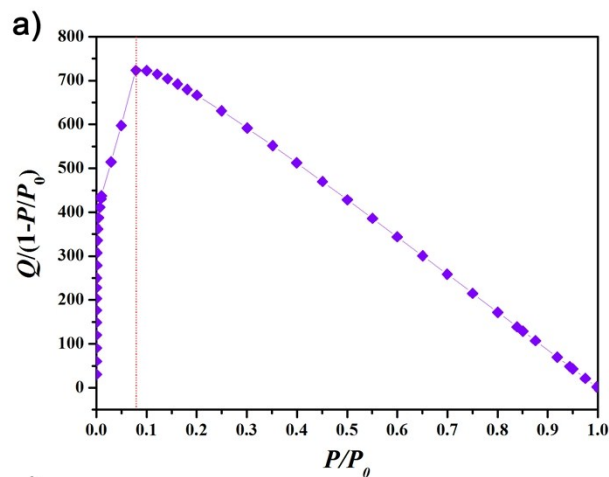Figure S1. The asymmetric structural unit of HHU-1.

Figure S2. PXRD patterns of HHU-1.

SECTION S3. BET Surface Area Analyses

P/P$_0$ Range	0.000465994 - 0.029452976
R^2	0.9953
C	769
V$_m$	526
1/(√C+1)	0.0348
P/P$_0$(V$_m$)	0.0292
Δ(P/P$_0$(V$_m$))	19.2
BET area	2290

Figure S3. BET area calculation for HHU-1 from simulated nitrogen isotherm at 77 K. a) Only points to the left of the dashed line are selected based on the first consistency criterion, b) Plot to select linear P/Po range: selected points are shown in white, the black line indicates the BET-calculated pressure corresponding to monolayer completion (1/(√C+1)), the cyan line indicates the pressure corresponding to the BET-calculated monolayer loading. c) The selected points and black and cyan lines from panel "b" are shown in the complete isotherm. The table contains all the information relevant to the BET consistency criteria.[1]

SECTION S4. Pore size distribution

Pore size distribution (PSD) was calculated from analysis of the Ar isotherm (adsorption branch) at 87 K using non-local density functional theory (NLDFT) implementing a hybrid kernel based on a zeolite/silica model containing cylindrical pores in the software package of Quantachrome AUTOSORB-1 automatic volumetric instrument.
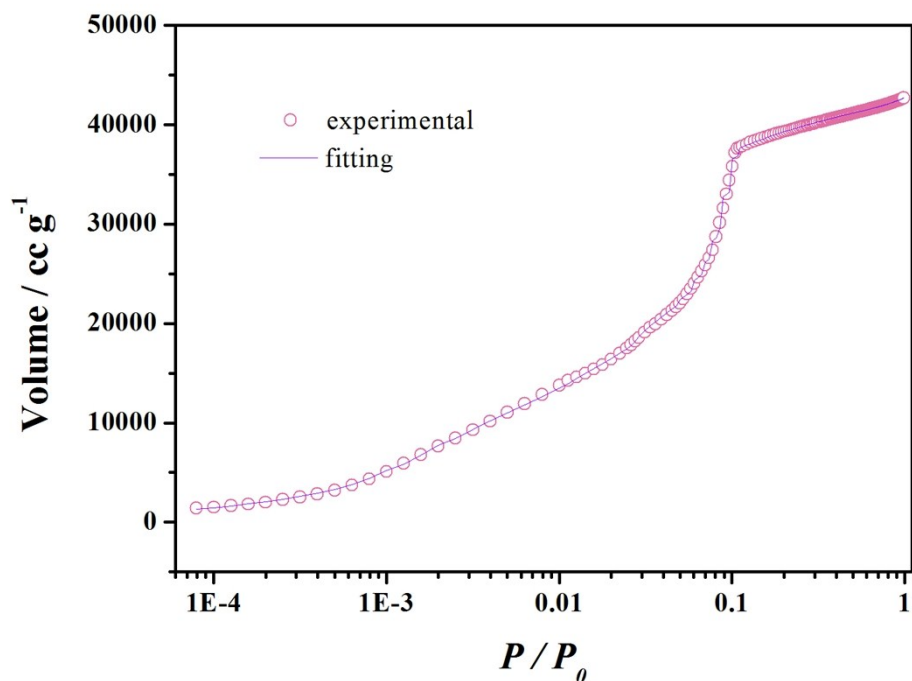

Figure S4. Comparison of the NLDFT fitting for the Ar adsorption isotherm with the experimental data of HHU-1. Fitting error: 0.325 %.

SECTION S5. Estimation of the isosteric heats of gas adsorption.

A virial-type[2] expression comprising the temperature-independent parameters a_i and b_i was employed to calculate the enthalpies of adsorption for CO_2 (at 273 and 298 K). The data were fitted using the equation:

$$\ln P = \ln N + 1/T \sum_{i=0}^{m} a_i N^i + \sum_{i=0}^{n} b_i N^i \quad (1)$$

Here, P is the pressure expressed in torr, N is the amount adsorbed in mmol/g, T is the temperature in K, a_i and b_i are virial coefficients, and m, n represent the number of coefficients required to adequately describe the isotherms (m and n were gradually increased until the

contribution of extra added a and b coefficients was deemed to be statistically insignificant towards the overall fit, and the average value of the squared deviations from the experimental values was minimized).

$$Q_{st} = -R\sum_{i=0}^{m} a_i N^i \quad (2)$$

Here, Q_{st} is the coverage-dependent isosteric heat of adsorption and R is the universal gas constant.
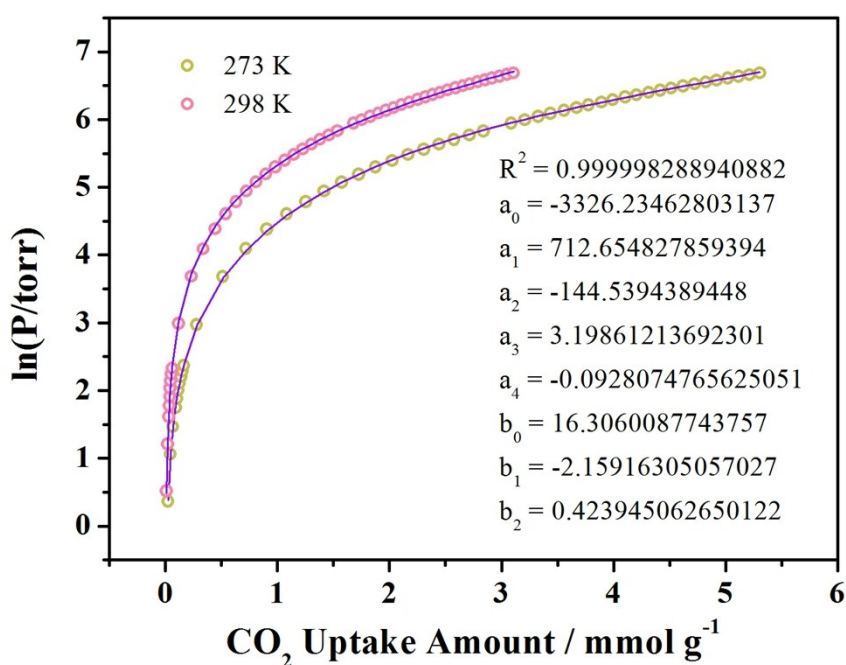

Figure S5. The details of virial equation (solid lines) fitting to the experimental CO_2 adsorption data (symbols) for NJU-Bai22.
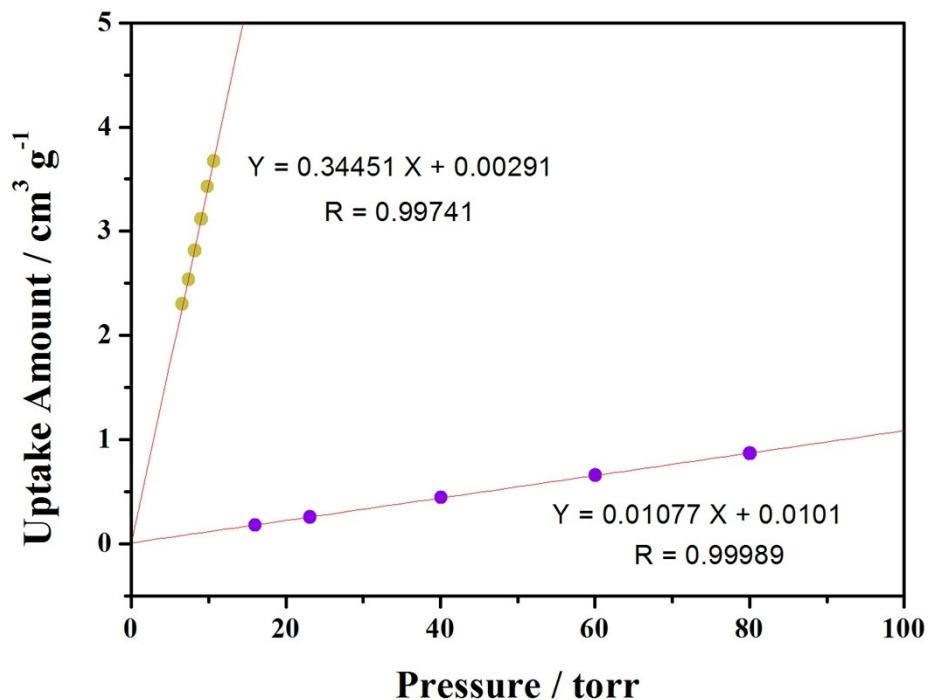
SECTION S6. Initial slop fitting

Figure S6. The fitting initial slope of CO_2 and N_2 isotherms for HHU-1 collected at 273 K.

SECTION S7. IAST adsorption selectivity calculation.

We adopt the ideal adsorbed solution theory (IAST) based upon the experimental single gas adsorption measurements, including carbon dioxide and nitrogen at 273 K, which is commonly used to predict binary mixture adsorption selectivity. Using the pure component isotherm fits, the adsorption selectivity is defined by

$$S_{ads} = \frac{q_1/q_2}{p_1/p_2} \qquad (3)$$

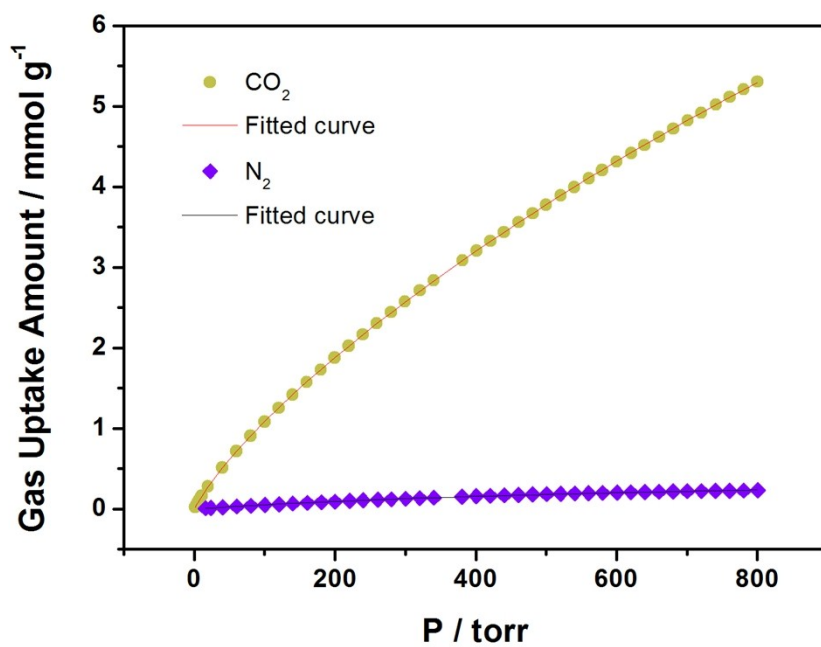where q_i is the amount of i adsorbed and p_i is the partial pressure of i in the mixture.

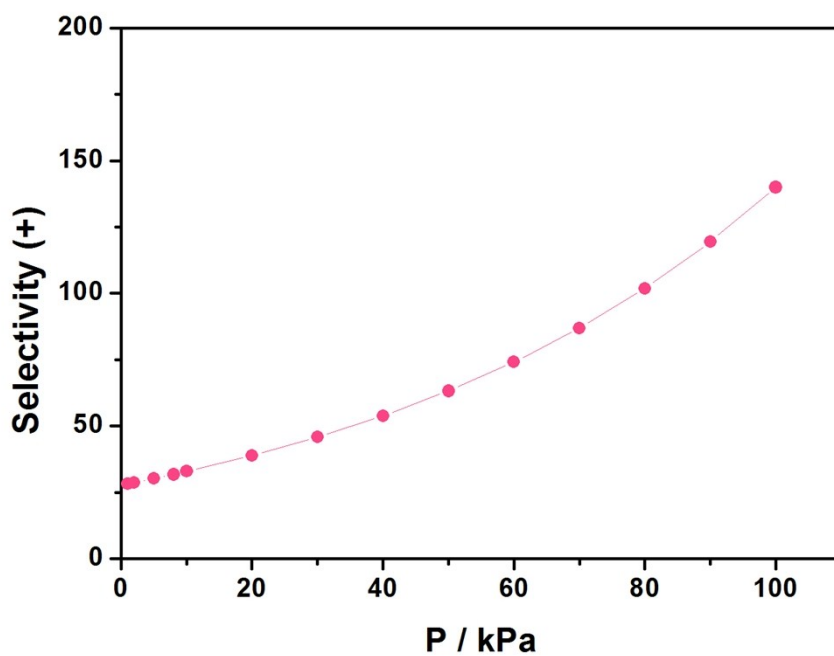Figure S7. CO_2 and N_2 uptakes of HHU-1 at 273K. Isotherms were fitted to a dual-site Langmuir equation

Figure S8. The CO_2/N_2 selectivity of HHU-1 at 273 K predicted by IAST
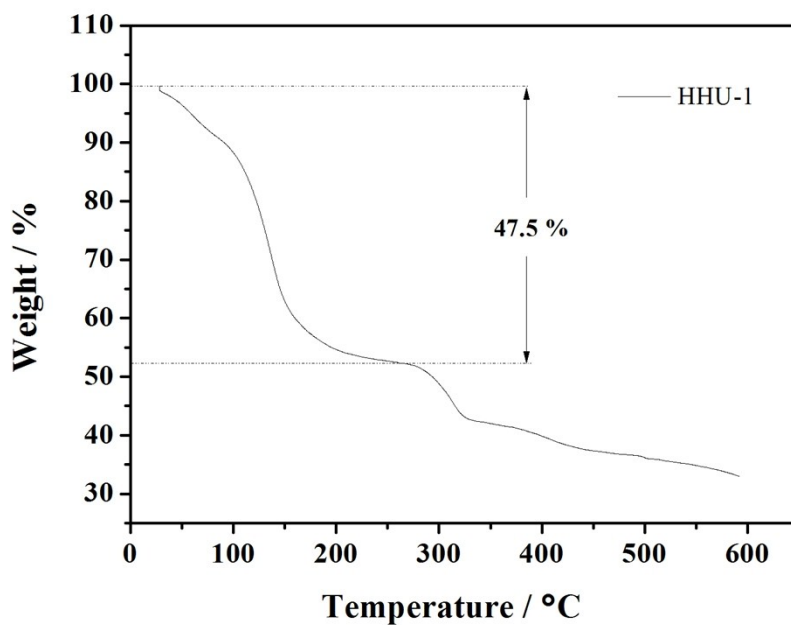
SECTION S8. Thermal stability.

Figure S9. TG curve of HHU-1.

References
1. (1) Rouquerol, J.; Llewellyn, P.; Rouquerol, F. In Studies in Surface Science and Catalysis; P.L. Llewellyn, F. R.-R. J. R., Seaton, N., Eds.; Elsevier: 2007; Vol. Volume 160, p 49; (2) Gomez-Gualdron, D. A.; Moghadam, P. Z.; Hupp, J. T.; Farha, O. K.; Snurr, R. Q. *J. Am. Chem. Soc.* **2016**, *138* (1), 215.
2. Rowsell, J. L. C.; Yaghi, O. M. *J. Am. Chem. Soc.* **2006**, *128*, 1304.